

High speed single photon detection in the near-infrared

Z. L. Yuan,* B. E. Kardynal, A. W. Sharpe, and A. J. Shields

*Toshiba Research Europe Ltd, Cambridge Research Laboratory,
208 Cambridge Science Park, Milton Road, Cambridge, CB4 0GZ, UK*

(Dated: February 1, 2008)

Abstract

InGaAs avalanche photodiodes (APDs) are convenient for single photon detection in the near-infrared (NIR) including the fibre communication bands (1.31/1.55 μm). However, to suppress afterpulse noise due to trapped avalanche charge, they must be gated with MHz repetition frequencies, thereby severely limiting the count rate in NIR applications. Here we show gating frequencies for InGaAs-APDs well beyond 1 GHz. Using a self-differencing technique to sense much weaker avalanches, we reduce drastically afterpulse noise. At 1.25 GHz, we obtain a detection efficiency of 10.8% with an afterpulse probability of 6.16%. In addition, the detector features low jitter (55 ps) and a count rate of 100 MHz.

PACS numbers: 85.60.Gz Photo detectors; 85.60.Gw Photodiodes; 03.67.Dd Quantum Cryptography

Near-infrared (NIR) single photon detection is required for quantum key distribution (QKD),¹ fibre optical sensing,² eye-safe ranging and timing,³ semiconductor device analysis,⁴ singlet oxygen detection,⁵ as well as photonic research in a wide range of disciplines. InGaAs/InP avalanche photodiodes (APDs) have proven a practical choice for wavelengths in the region 1.0–1.7 μm .^{6,7,8,9,10} However, the performance of these devices lags far behind that of silicon APDs, used for visible photon detection, due to greater defect density in III-V semiconductor devices.

An APD detects a single photon through avalanche multiplication of a photon-excited carrier, resulting in a detectable macroscopic current flow. However, avalanche carriers that are trapped by defects, and then subsequently spontaneously released, can induce a second spurious avalanche, contributing to the erroneous count noise. To suppress the rate of these afterpulses, InGaAs APDs are normally gated with only MHz frequencies with each active gate lasting for a few nanoseconds. Furthermore, a dead time of a few microseconds,⁸ has to be applied following each photon detection to allow the trapped carriers time for decay. These considerations limit the maximum count rate of an APD to typically just ~ 100 kHz.⁹ This has rendered InGaAs APDs unsuitable for applications, which require high-speed single photon detection, such as next generation high bit rate QKD.^{11,12,13}

Alternative technologies, such as upconversion with periodically poled LiNbO₃ (PPLN)¹⁴ and superconducting nanowire detectors,¹⁵ have been developed. However, those PPLN upconversion detectors^{12,13} suffer from high background photon count rate and require sophisticated optical alignment for noise rejection, while superconducting device requires cryogenic cooling to temperatures of around a few K.

In this paper, we show gating frequencies for InGaAs-APDs well beyond 1 GHz. Using a self-differencing technique to sense much weaker avalanches, we reduce drastically the avalanche charge and hence the afterpulse noise. At 1.25 GHz, we obtain a detection efficiency of 10.8% with an afterpulse probability of 6.16%. In addition, the detector features low timing jitter (55 ps) and a count rate of 100 MHz, and does not require cryogenic cooling. These features make the device suitable for a wide range of applications requiring high count rate, low noise, fast NIR single photon detection.

The key to improve InGaAs APD speed is to limit the avalanche charges by detecting weak avalanches. Unfortunately, weak avalanche signals are often buried within the APD capacitive response, especially when using fast gating signals. Figure 1(b) plots an APD

response, recorded on an oscilloscope with 100-ps rise time resolution, to a series of 0.62 GHz square wave voltage gating pulses (Fig. 1(a)). In response to each gate, the APD produces a positive peak, followed by a negative peak, due to the charging and subsequent discharging of the finite capacitance of the APD. No avalanche signals can be identified in this waveform. However, numerically subtracting a signal that is identical to Fig. 1(b) but shifted by one gating clock as shown in Fig. 1(c), the resulting waveform (Fig. 1(d)) shows clearly a distinctive positive peak, followed by a negative peak separated by one clock period. The positive peak and the following negative one revealed here is attributed to an avalanche. By discriminating either the positive or negative peaks, avalanches, previously completely buried within the capacitive response, become detectable. Note that the amplitude of the avalanche signal is 10 times weaker than the APD capacitive response and is superimposed on the negative capacitive peak. Without removing the capacitive response, an avalanche would have to be at least 20 times stronger in order to be detected.

Numerical subtraction is rather impractical, especially when the gating frequency is high. In practice, such an operation may be realized using hardware. Figure 1(e) shows a self-differencing circuit designed for operation that is equivalent to the numerical subtraction described above. It consists of a 50/50 pulse splitter to divide the APD response into two equal components, which are then combined by a differencer. The coaxial cables connecting the splitter and the differencer have different lengths to induce a delay of one gating period between two components. Thus, the output of the self-differencer is the difference between two identical waveforms shifted relatively by one gating period. A 21 dB suppression of the APD capacitive response is achieved with the circuit. Figure 1(f) shows a detectable avalanche as a result of self-differencing.

The InGaAs APD under test was cooled electrically to -30°C . It was gated using a square wave signal generated by a pulse generator. The APD output, after passing through the self-differencer, is pulse-shaped using a discriminator before analysis by a pulse counter or a time-correlated photon counter. To characterize its detection efficiency, the APD was illuminated with 80-ps long pulses of 1550 nm light from a distributed feedback laser diode, which was synchronized at $1/64$ of the APD gating frequency. Each pulse was attenuated to 0.1 photons per pulse before coupling into the APD fibre pigtail. The setup is suitable for measuring the detection efficiency, dark count and afterpulse probabilities.

We first tested whether the InGaAs APD detects single photons by scanning the laser

pulse delay. The APD was biased at 1.4 V below its breakdown voltage of 47.3 V, and gated by a superimposed 0.62 GHz square wave with an amplitude of 6.6 V. As shown in Fig. 2(a), where the photon count rate is plotted as a function of the laser pulse delay, photons are detected only when they arrive within the gate duration defined by the applied square wave. Photons arriving between the gates are not detected, evidenced by the fact that the count rate falls to the dark count level. The full width at half maximum (FWHM) of the photon detection peak is 170 ps, significantly narrower than the gate width (800 ps), suggesting that the APD active duration is much smaller than the electrical gate.

Figure 2(b) shows a time-resolved histogram of photon arrivals when the laser delay was tuned to maximize count rate. As the laser diode was triggered at the 1/64 of the gating frequency, the peak at 0 ns corresponding to the illuminated gate is much stronger than the remaining peaks corresponding to the non-illuminated gates. The photon-induced peak is very sharp, with a FWHM of 55 ps, indicating extremely low detection jitter. Adjacent peaks are well separated with a >700 ps gap within which no counts were registered.

The histogram of dark counts is shown in Fig. 2(c), measured with the laser switched off. The count rate is much lower for each gate than recorded for non-illuminated gates (Fig. 2(b)) with the laser on, suggesting that under illumination afterpulses are the dominant noise source. The afterpulse probability P_A , defined here as the ratio of the total afterpulse counts to the photon counts, can be obtained from

$$P_A = \frac{(I_{NI} - I_D) \cdot R}{I_{Ph} - I_{NI}} \quad (1)$$

where I_{Ph} and I_{NI} are the count rate per gate at the illuminated and non-illuminated gates respectively, while I_D is the dark count rate for each gate. $R = 64$ is the ratio of the gating frequency to the laser pulse frequency.

The afterpulse probability was measured as a function of the photon detection efficiency, which was varied by tuning the DC bias level in the range of 45.5 — 47.0 V. The square wave amplitude was fixed at 6.6 V for a gating frequency of 0.62 or 0.98 GHz, and at 4.6 V for 1.25 GHz. In Fig. 3(a), P_A is plotted as a function of the net detection efficiency η (excluding the dark and afterpulse counts). P_A generally increases with η , consistent with the greater avalanche charge flow at the higher bias required for higher detection efficiencies. There appears to be a critical efficiency η_c , below which P_A is less than 6.2% and changes slowly with η . When $\eta > \eta_c$, P_A increases sharply. It is found that $\eta_c \doteq 21\%$ for 0.62 GHz

TABLE I: Performance comparison of the self-differencing InGaAs APD with the PPLN upconversion detectors.

	η	P_D	η/P_D	Max (MHz)
InGaAs APD	10.9%	2.34×10^{-6}	4.6×10^4	100
PPLN ^a	1.2%	7×10^{-6}	1.71×10^3	15
PPLN ^b	3.6%	1.95×10^{-5}	1.85×10^3	15

^aReference 12

^bReference 13

and becomes notably lower at $\sim 11\%$ for 0.98 GHz and 1.25 GHz. It could well suggest that afterpulse noise is more prominent at higher gating frequencies. However, this may not be the case because η may be underestimated for high frequencies, due to the comparable duration of the optical active gate and the laser pulse duration.

Figure 3(b) plots the dark count probability P_D as a function of η . As usual, P_D increases with η . At $\eta \approx 11\%$, the dark count probability is similar for all gating frequencies, at $\sim 2.5 \times 10^{-6}$ per gate. Such a dark count probability is very low indeed, considering the operation temperature of -30°C . It is roughly 20 times less than obtained previously using conventional discrimination.¹⁶

The detector linearity and maximum achievable count rate were also studied. In this experiment, a standard telecom direct modulation laser diode was used to illuminate the APD at the same rate as the APD gating. The relatively wide optical pulse (250 ps FWHM) resulted in an effectively lower photon detection efficiency. As shown in Fig. 4, the count rate increases linearly with the photon flux over > 30 dB dynamical range. The increase in photon count rate is sub-linear for count rates exceeding 20 MHz, and finally saturates at 100 MHz. The count rate here is more than two orders of magnitude higher than previously achieved.⁹ Moreover, the saturation rate is limited by the pulse-shaping electronics, rather than the detector, and could be increased further by using faster electronics.

Finally we compare the performance of the self-differencing APD with PPLN upconversion detectors using Si detectors.^{12,13} As summarized in Table I, the self-differencing APD shows significantly better detection efficiency and dark count probability P_D . It is

also polarization independent and sensitive to a broad spectrum of photons while an up-conversion detector only detects photons at a fixed wavelength with a particular polarization due to stringent phase matching requirement. Moreover, the self-differencing APD features 100 MHz maximum count rate, as compared with ~ 15 MHz for an up-conversion detector,¹⁷ making it more attractive for high bit rate QKD. Besides improved performance, gated operation is another advantage for QKD. Gated operation automatically rejects background photons arriving between gates. As demonstrated in Fig. 2(a) the APD active width is only 170 ps, far less than the gating period of 1.6 ns, suggesting $\sim 90\%$ rejection of background photons. Of course, gated operation requires clock synchronization, however, even more precise synchronization is required for the up-conversion detectors based QKD where post-measurement gating¹³ is required for noise rejection. One possible drawback for the self-differencing detector is that it does not allow tuning the gating frequency continuously over a wide range, as the frequency is determined by the length difference of two co-axial cables used. It is found that, within $\pm 0.5\%$ of the central gating frequency, the self-differencing circuit cancels the capacitive responses well and no degradation in photon counting performance was observed. Such a tuning range makes it suitable for many applications, such as QKD, for which the clock frequency has typically much better stability than $\pm 0.5\%$.

In conclusion, we have demonstrated for the first time practical GHz single photon detection at 1550 nm using a self-differencing InGaAs APD.

* Electronic address: zhiliang.yuan@crl.toshiba.co.uk

- ¹ C. H. Bennett and G. Brassard, Proceedings of the IEEE International Conference on Computers, Systems and Signal Processing, Bangalore, India, 1984, pp. 175-179.
- ² J. M. Lopez-Higuera, *Handbook of Optical Fibre Sensing Technology* (Wiley, Chichester, 2002).
- ³ T. Maruyama, F. Narusawa, M. Kudo, and M. Tanaka, Opt. Eng. **41**, 395(2002).
- ⁴ R. Ispasoiu, T. Crawford, B. Johnston, C. Shaw, S. Kasapi, J. Goertz, O. Rinaudo and P. Ouimet, Microelectronics Reliability **46**,1504(2006).
- ⁵ O. Shimizu, J. Watanabe, K. Imakubo, and S. Naito, Chem. Lett. **19**, 203(1997).
- ⁶ A. Lacaita, F. Zappa, S. Cova, and P. Lovati, Appl. Opt. **35**, 2986(1996).
- ⁷ A. Tomita and K. Nakamura, Opt. Lett. **27**, 1827(2002).

- ⁸ D. S. Bethune, W. P. Risk and G. W. Pabst, J. Mod. Opt. **51**, 1359(2004).
- ⁹ A. Yoshizawa, R. Kaji and H. Tsuchida, Japanese J. Appl. Phys. **43**, L735(2004).
- ¹⁰ N. Namekata, S. Sasamori, and S. Inoue, Opt. Express **14**, 10043(2006).
- ¹¹ K. J. Gordon, V. Fernandez, G. S. Buller, I. Rech, S. D. Cova, and P. D. Townsend, Opt. Express **13**, 3015(2005).
- ¹² R. T. Thew, S. Tanzilli, L. Krainer, S. C. Zeller, A. A. Rochas, I. Rech, S. Cova, H. Zbinden, and N. Gisin, New J. Phys. **8**, 32(2006).
- ¹³ E. Diamanti, H. Takesue, C. Langrock, M. M. Fejer, and Y. Yamamoto, Opt. Express **14**, 13073(2006).
- ¹⁴ M. A. Albota and F. N. C. Wong, Opt. Lett. **29**, 1449(2004).
- ¹⁵ R. H. Hadfield, J. L. Habif, J. Schlafer, R. E. Schwall, and S. W. Nam, Appl. Phys. Lett. **89**, 241129(2006).
- ¹⁶ Z. L. Yuan, A. W. Sharpe, and A. J. Shields, Appl. Phys. Lett. **90**, 011118(2007).
- ¹⁷ No maximum count rate of PPLN upconversion detectors has been reported, and the value here is inferred from the performance of Si-APD single photon detectors. See: Datasheet, SPCM-AQR Single Photon Counting Module, PerkinElmer.

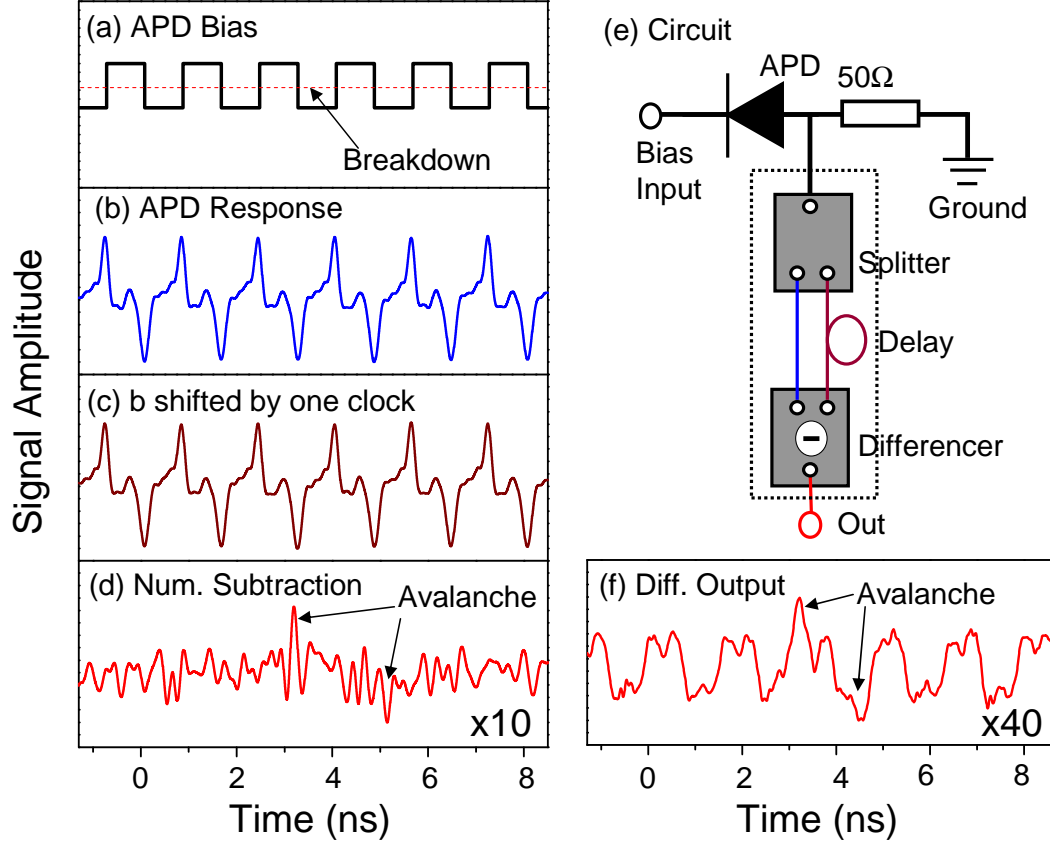


FIG. 1: (a) A series of biasing square wave gates (solid line) applied to an APD; The dashed line indicates the APD breakdown voltage. (b) An APD response to the square wave gates, recorded by an oscilloscope; The APD here was gated with a continuous 0.62 GHz square wave. Note that no avalanche is visible. (c) Same response as (b), but shifted by a clock period; (d) Numerical subtraction $\mathbf{b}-\mathbf{c}$, leaving the avalanche signal visible; Vertical scale in (d) is scaled up by a factor of 10 as compared to (b) and (c) for clarity. (e) An electrical circuit to realize the self differencing; (f) Output of the self-differencer recorded by an oscilloscope. Vertical scale here is scaled up by a factor of 40.

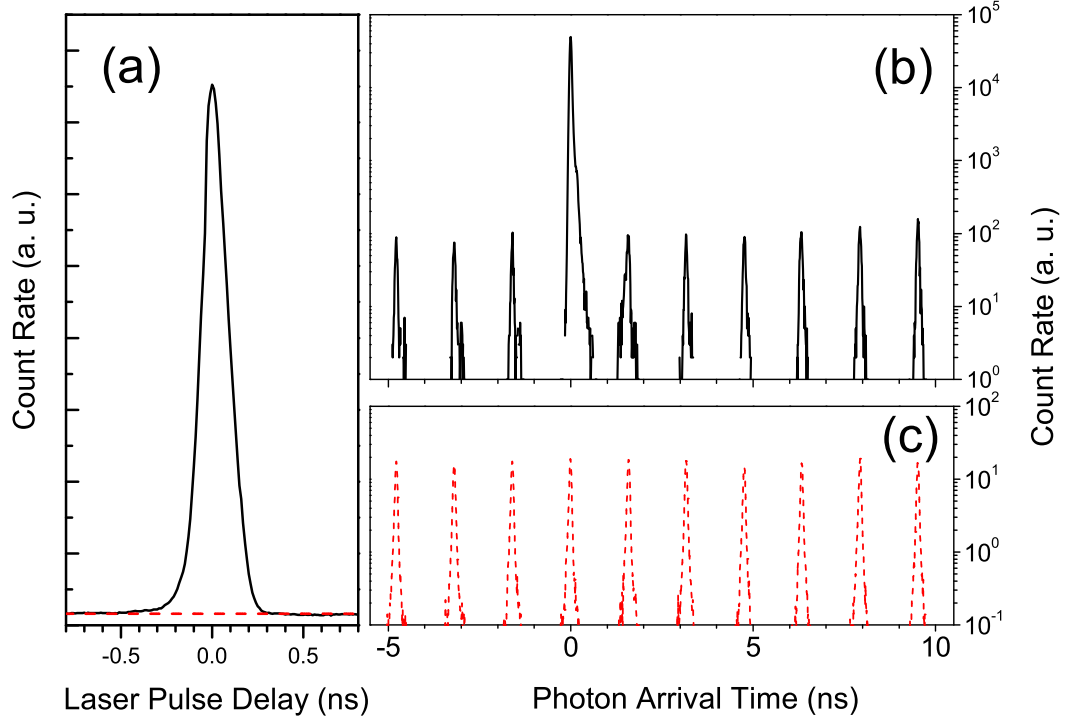


FIG. 2: (a) Photon count rate (solid line) as a function of the laser pulse delay; The dashed line indicates the detector dark count rate. (b) Time-resolved photon arrival time histogram under illumination; (c) Time-resolved histogram of dark counts under no illumination. The APD here was gated at 0.62 GHz.

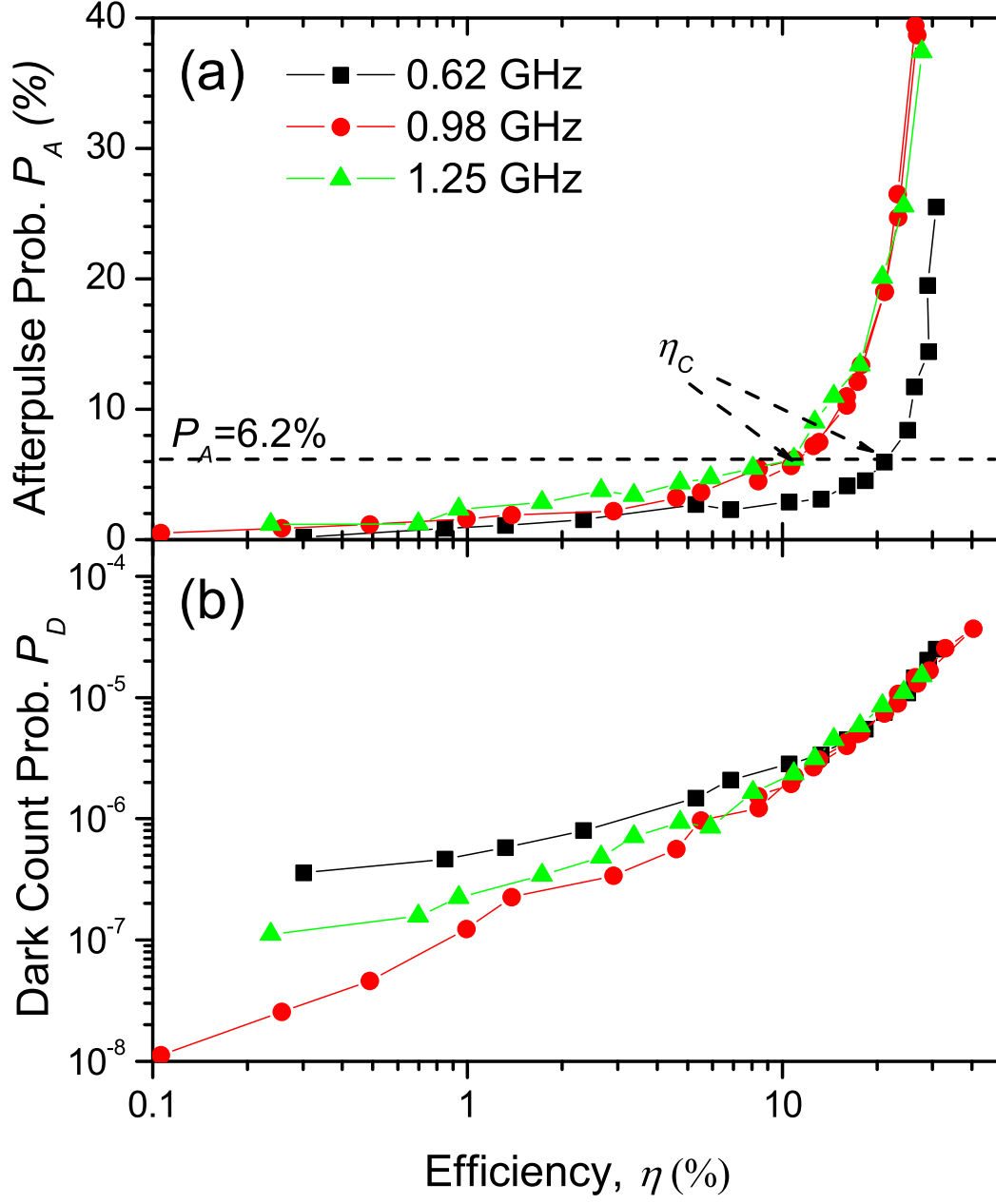


FIG. 3: (a) Detector afterpulse probability P_A , and (b), dark count probability P_D as a function of the net detection efficiency η .

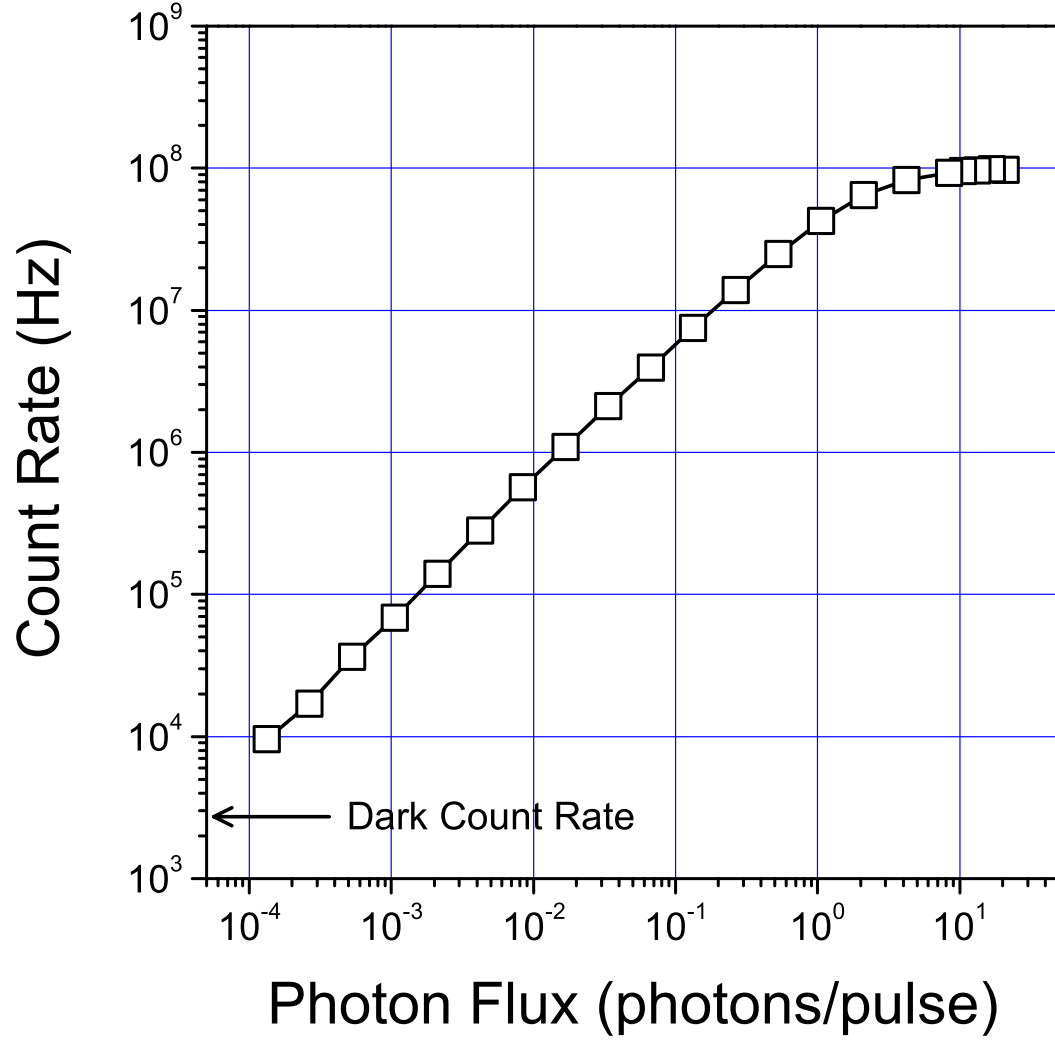


FIG. 4: Photon detection rate as a function of photon flux. 0.98 GHz gating was used for this measurement. The arrow indicated the detector dark count rate of 2.8 kHz, which was subtracted from the measured results.